Structural Engineering and Mechanics, *Vol. 75, No. 4 (2020) 497-506*
DOI: https://doi.org/10.12989/sem.2020.75.4.497

Study on vibration energy characteristics of vehicle-track-viaduct coupling system considering partial contact loss beneath track slab

Linya Liu*, Zhiyuan Zuo[a], Qinyue Zhou[b], Jialiang Qin[c] and Quanmin Liu[d]

Engineering Research Center of Railway Environment Virbration and Noise, Ministry of Education, East China Jiaotong University, Nanchang 330013, China

(Received January 2, 2020, Revised February 16, 2020, Accepted February 22, 2020)

Abstract. CA mortar layer disengagement will give rise to the overall structural changes of the track and variation in the vibration form of the ballastless track. By establishing a vehicle-track-viaduct coupling analysis and calculation model, it is possible to analyze the CRTS-I type track structure vibration response while the track slab is disengaging with the power flow evaluation method, to compare the two disengaging types, namely partial contact loss at one edge beneath track slab and partial contact loss at midpoint beneath track slab. It can also study how the length of disengaging influences the track structures vibration power. It is showed that when the partial contact loss beneath track slab, and the relative vibration energy level between the rail and the track slab increases significantly within [10, 200]Hz with the same disengaging length, the partial contact loss at one edge beneath track slab has more prominent influence on the vibration power than the partial contact loss at midpoint beneath track slab. With the increase of disengaging length, the relative vibration energy level of the track slab grows sharply, but it will change significantly when it reaches 1.56 m. Little effect will be caused by the relative vibration energy level of the viaduct. The partial contact loss beneath the track slab will cause more power distribution and transmission between the trail and track slab, and will then affect the service life of the rail and track slab.

Keywords: high-speed railway; vibration energy; dynamic compliance method; Contact Loss Beneath Track slab

1. Introduction

In China's transportation network, high-speed railway (HSR) plays an increasingly significant role because of its convenient, stable, and efficient transportation efficiency (Zhu *et al*. 2018). Domestic HSR adopts a viaduct and plate-type ballastless track structure because the principal function of the bridge is to provide smooth and stable over-bridge lines for high-speed trains, thus ensuring the safe and comfortable operation of trains (Sun *et al*. 2014, Dai *et al*. 2018). The plate-type ballastless track structure has high stability and durability and can well control the uneven settlement of the track foundation (Thompson and Verheij 1997, Song *et al*. 2012). The slab ballastless track structure under high-frequency loads, ambient temperature, and other factors, however, no longer maintains continuous contact with the surface of the mortar in a local area. The track slab vacated, which could induce a sharp increase in the vibration response of the track structure and affect the service life of the track (Liu *et al*. 2019a). The CRTS-I type track structure laying shows many voids in China (Ren *et al*. 2014). And it becomes critical to study the effect of the slab ballastless track on the vibration response of the track structure.

Some scholars conducted some research on the issue of orbital slab-emptying at home and abroad. For instance, Kaewunruen (2007) established a finite element (FE) model to analyze the vertical vibration mode of the sleeper when the sleeper produced a gap. Liu (Li *et al*. 2014) established a vehicle-track-viaduct FE model and analyzed the dynamic response of the vehicle, track displacement, and acceleration under different plate-end void lengths through dynamic software. Ren (Ren *et al*. 2016, Ren *et al*. 2020) established a carriage rail-subgrade model to analyze the stress response of CA mortar lamination under different void lengths. Wang (Xu *et al*. 2017) analyzed the stress conditions and fatigue life under the voiding and deterioration of two types of CA mortars in the slab ends and slabs of the I-type track slab using the miner linear fatigue criterion.

The research on the partial contact loss beneath the track slab phenomenon is mostly based on the analysis of single indexes such as displacement and acceleration. When partial contact is lost beneath the track slab, it will cause the redistribution of the vibration energy of the track structure, resulting in changes in the specific values of energy transfer, storage, and dissipation in the various layers (Li *et al*. 2010, Fu *et al*. 2018). Furthermore, when the vibration energy is concentrated near the disengaging of the track slab, it will cause further damage after reaching a certain limit. The CRTS-I type slab ballastless track is used as an example to deeply investigate the influence of partial contact loss beneath the track slab on the vibration energy

*Corresponding author, Professor
E-mail: lly@ecjtu.edu.cn
[a] M.Sc. Student
E-mail: 2017018082301009@ecjtu.edu.cn
[b] M.Sc. Student
E-mail: 2017018082301003@ecjtu.edu.cn
[c] Ph.D. Student
E-mail: qjl@ecjtu.edu.cn
[d] Associate Professor
E-mail: liuquanmin@ecjtu.edu.cn

http://www.techno-press.com/journals/sem&subpage=7
ISSN: 1225-4568 (Print), 1598-6217 (Online)

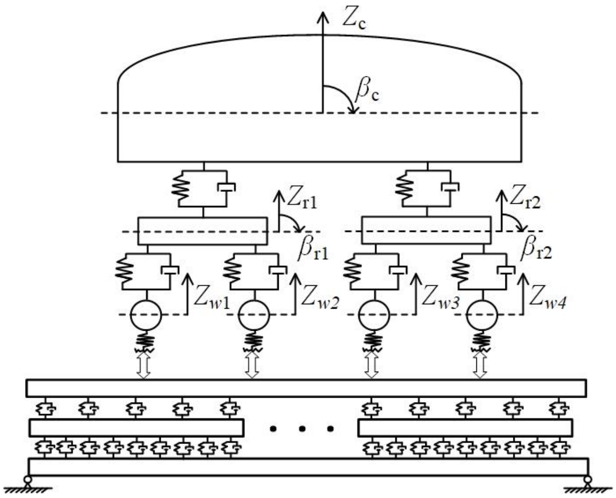

Fig. 1 Vehicle-Track-Viaduct coupling analysis and calculation model

characteristics of the vehicle-track-viaduct coupling system. The vehicle-track-viaduct coupling analysis and calculation model is established to compare and analyze the vibration energy distribution and transmission of the track structure under the evacuation of the track slab of different lengths by dynamic flexibility methods. It aims to provide a reference for the repairing work of the track slab after the evacuation disease.

2. Theory of vehicle-track-viaduct coupling analysis and calculation model

Based on the dynamic flexibility method, the researcher established a power flow model of the vehicle-track-viaduct coupling dynamic system. The vehicle-track-viaduct coupling dynamic system consists of a vehicle subsystem and ballastless track-viaduct structure subsystem, linked by a spatial wheel-rail contact geometry relationship and wheel-rail force (Fenander 1997, Schulte-Werning *et al*. 2006). The vehicle subsystem consists of the carriage body, bogie, and wheels, which are connected by secondary suspension and primary suspension. The single carriage model has 10 degrees of freedom, and dynamic flexibility of carriage is calculated. The rail is simplified to be an infinite length Timoshenko beam. The track slab is simplified to a discretized free-free Euler-Bernoulli beam, and the viaduct is simplified to be a supported Euler beam. Fasteners and the CA mortar are simulated by linear elastic damping elements (Liu *et al*. 2009, Shi *et al*. 2017). The model is shown in Figure 1

2.1 Vehicle subsystem

According to the traits of the wheel-rail contact, wheel-rail interaction coupling used linearized wheel-rail contacting stiffness. The irregularity spectrum is taken with the rail roughness amplitude limit from GB/T 5111-2011 (Song *et al*. 2018), and its ride comfort is significant. Tracking irregularities give vertical excitation to wheel-rail contact, resulting in a harmonic response of the carriage, which brings harmonic response into the vibration equation of the carriage; the vibration relation of the carriage excited by track irregularity is expressed as:

$$\{Z_{\mathrm{v}}(\omega)\} = \frac{\{P_{\mathrm{v}}(\omega)\}}{-\omega^2[M_{\mathrm{v}}] + i\omega[C_{\mathrm{v}}] + [K_{\mathrm{v}}]} \quad (1)$$

where $\{P_v(\omega)\}$ means the amplitude of vertical wheel-rail interaction forces caused by track irregularities, and $\{Z_v(\omega)\}$ represents the amplitude of the displacement amplitude of the vehicle subsystem.

2.2 Ballastless rail-viaduct structure subsystem

The ballastless rail-viaduct structure contains rail, track slab, and viaduct. The fasteners connect the rail and the track slab, and the track slab and viaduct are connected by the CA mortar among them. Figure 2 shows the flowchart of the subsystem establishment.

The rail is simplified to an infinite length Timoshenko beam, and the relation of dynamic flexibility methods are as follows (Carlone and Thompson 2001, Song *et al*. 2018, Liu *et al*. 2019b):

$$\beta_r(x_1,x_2) = \left(u_1 e^{-ik_1|x_1-x_2|} + u_2 e^{-k_2|x_1-x_2|}\right) \quad (2)$$

where $\beta_\gamma(x_1, x_2)$ means the displacement at x_1 caused by the unit harmonic load at x_2 in the rail. k_1, k_2, u_1, u_2 denote coefficients related to the rail parameters (Hamet 1999, Liu *et al*. 2019c, d).

The rail mainly bears vehicle load P and fastener load F_f. The displacement expression in the frequency domain follows:

$$z_r(x) = \sum_{w=1}^{N_w} \beta_r(x,x_w) P_w - \sum_{n=1}^{N} \beta_r(x,x_n) F_{fn} \quad (3)$$

where P_ω denotes wheel vertical force applied by the w^{th} wheel pair at x_ω of the rail. N_ω means the total number of wheels. F_{fn} means the support reaction applied by the n^{th} fastener to the rail of position x_n, and N indicates the total number of fasteners at a single rail.

Track slab is simplified to the free-free Euler-Bernoulli beam with finite length. The relation of dynamic flexibility method follows:

$$z_s(x) = \sum_{n=1}^{N} \beta_s(x,x_n) F_{fn} - \sum_{m=1}^{M} \beta_s(x,x_m) F_{jm} \quad (4)$$

where F_{jm} means support reaction applied by the m^{th} elastic damping elements of the CA mortar layer discretization to the track slab of position x_m, and M denotes the number of all elastic damping elements at CA mortar layer discretization.

The dynamic flexibility of multiple track slabs of the viaduct could be obtained by the dynamic flexibility of a single, track slab can be expressed as

$$\beta_s = diag\left[[\beta_{s1}]_1 [\beta_{s1}]_2 [\beta_{s1}]_3 \cdots [\beta_{s1}]_n\right] \quad (5)$$

where β_{s1} means the dynamic flexibility of a single track slab.

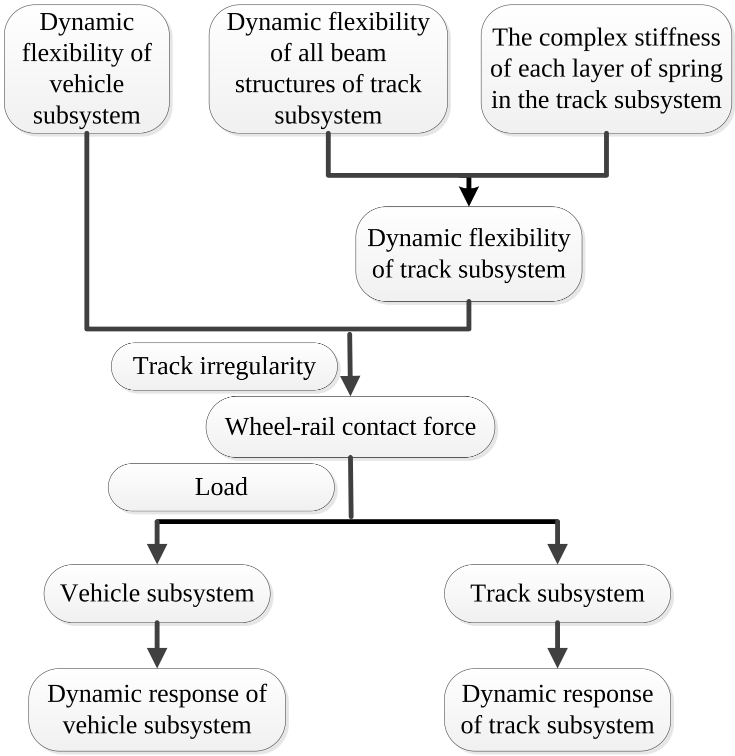

Fig. 2 Flowchart for establishing vehicle-track-viaduct coupling analysis and calculation model

Viaduct simulation using simple-supported Euler beams, the dynamic flexibility method follows:

$$z_b(x) = \sum_{n=1}^{N} \beta_b(x,x_n) F_{jm} - \sum_{h=1}^{2} \beta_b(x,x_{zh}) F_{zh} \tag{6}$$

where F_{zh} means the support reaction applied by the h^{th} viaduct bearing to the viaduct of position x_{zh}.

By combining equations (4), (5), and (6), the numerical relationship between the frequency response of the ballastless rail-viaduct structure and the vehicle load can be derived. expressed as:

$$\{P\} = [\beta K]\{Z\} \tag{7}$$

where $[\beta K]$ is composed of the dynamic flexibility of the ballastless rail-viaduct structure multiplied by the complex stiffness. $\{Z\}$ consists of the displacements of each structure of the ballastless rail-viaduct structure, and $\{P\}$ is the load matrix of the wheel-rail force on the ballastless rail-viaduct structure.

2.3 Evaluation ındexes of vibration energy

The displacement response of the rail, track slab, and viaduct in the ballastless rail-viaduct structure is calculated by Equation (7). Subtracting displacements from the adjacent parts, the corresponding internal force can be calculated as F_{fn}, F_{jm}, F_{zh}:

$$\begin{cases} F_{rn} = K_f\left(Z_r(x_n) - Z_s(x_n)\right) \\ F_{sm} = K_j\left(Z_s(x_m) - Z_b(x_m)\right) \\ F_{zh} = K_z Z_b(x_h) \end{cases} \tag{8}$$

Based on the power flow theory, the vibration energy transmitted to each part is P_{rn}, Psm, Pzh:

$$\begin{cases} P_{rn}(w) = \dfrac{1}{2}\mathrm{Re}\left(F_{fn}(w)^* V_{rn}(w)^*\right) \\ P_{sm}(w) = \dfrac{1}{2}\mathrm{Re}\left(F_{sm}(w)^* V_{sm}(w)^*\right) \\ P_{zh}(w) = \dfrac{1}{2}\mathrm{Re}\left(F_{zh}(w)^* V_{zh}(w)^*\right) \end{cases} \tag{9}$$

where *Re* means that the real part calculation will be selected, and * means that the conjugate calculation will be selected.

When the train passes the section where the partial contact loss beneath the track slab occurs, the energy transferred layer-by-layer along the track structure will change. To comprehensively evaluate the changes in the vibration energy of the track structure and its vertical transmission when partial contact is lost beneath the track slab, the energy corresponding to all nodes contained in the three-layer track structure of the rail, track slab and viaduct must be summed:

$$\begin{cases} P_{rn}(w) = \dfrac{1}{2}\sum_{n=1}^{N}\mathrm{Re}\left(F_{fn}(w)^* V_{rn}(w)^*\right) \\ P_{sm}(w) = \dfrac{1}{2}\sum_{m=1}^{M}\mathrm{Re}\left(F_{sm}(w)^* V_{sm}(w)^*\right) \\ P_{zh}(w) = \dfrac{1}{2}\sum_{h=1}^{2}\mathrm{Re}\left(F_{zh}(w)^* V_{zh}(w)^*\right) \end{cases} \tag{10}$$

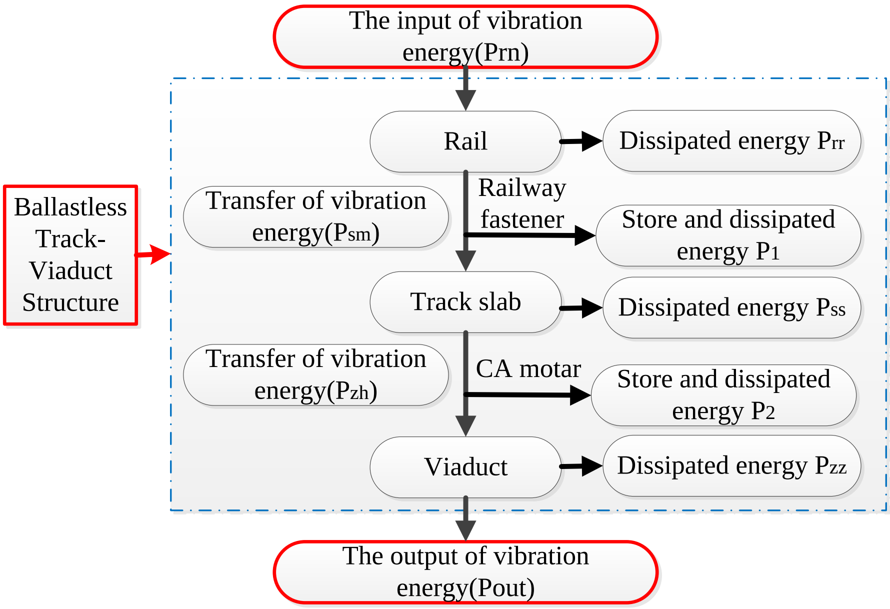

Fig. 3 Flowchart of vibration energy transfer process in ballastless rail-viaduct structure

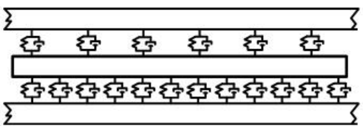

(a) Normal Condition

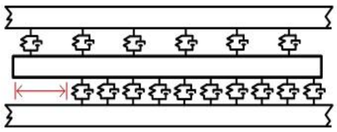

(b) Partial contact loss at one edge beneath track slab

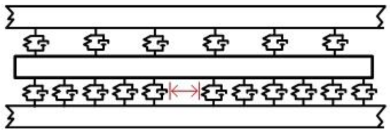

(c) Partial contact loss at midpoint beneath track slab

Fig. 4 Calculation condition

After obtaining the total vibration energy corresponding to each layer of the track structure to visually express and compare the energy change trend under different working conditions, this study performs an analysis using a relative vibration energy level and vibration energy transfer rate. Figure 3 shows the flowchart of the energy transfer of the power flow in the track structure.

Relative vibration energy level follows:

$$P_l(w) = 20\lg\left(\frac{P((w))}{P_0}\right) \tag{11}$$

where $P((\omega))$ denotes the total power flow in a certain layer of the track structure when the frequency is ω. P_0 means the reference power flow because the bottom of the track structure is a viaduct, so the value is $P_0=1\times10^{-8} N\bullet m/s$.

Vibration energy transfer rate:

$$P_{rs}(w) = \frac{P_r(w)}{P_s(w)} \tag{12}$$

where $P_r(\omega)$ denotes the relative vibration energy level of the rail layer, and $Ps(\omega)$ means the relative vibration energy level of the track slab layer. The vibration energy transfer rate between the track slab and the viaduct is the same as this formula. The vibration energy transfer rate reflects the proportion of vibration energy transferred in the track structure when it is transferred from one layer to the next. If the calculated rate is larger, it reflects that more energy is transferred between the two layers.

3. Influence of partial contact loss beneath the track slab on vibration energy of the track structure

3.1 Model parameters

Based on the established vehicle-track-viaduct coupling model, the vibration energy distribution and transmission of the ballastless rail-viaduct subsystem at contact loss beneath track slab are analyzed. This study takes a CRH3 high-speed train, CRTS-I type ballastless track plate, and a HSR box girder viaduct as instance. Table 1 shows the structural parameters.

3.2 Type of partial contact loss beneath the track slab

Two types of partial contact loss beneath the track slab for HSR ballastless tracks exists, namely partial contact loss at one edge beneath track slab and partial contact loss at midpoint beneath track slab (Ren *et al*. 2014). This study analyzes the effects of the two types of partial contact loss beneath the track slab on the track structure. The partial contact loss beneath the track slab manifests as the local CA mortar and the track slab no longer maintains continuous contact, so it cannot provide a vertical supporting force. When the CA mortar is completely evacuated along the longitudinal direction of the track line (lateral direction in the Figure 4), the overall impact on the system is the greatest. In this case, the form of the wheel-rail excitation

Table 1 Parameters of Track Structural

Parts	Projects	Values
Rail	Youngs modulus/(N/m^2)	2.1e11
	Moment of Inertia/(m^4)	3.217e-5
	Density/(kg/m^3)	7850
	Section area/(m^2)	7.745e-3
	Shear Modulus/(N/m^2)	7.7e10
Fasteners	Distance between fasteners/(m)	0.625
	Loss Factor	0.25
	Stiffness /(Pa)	5e7
CA Mortar	Stiffness /(Pa)	3.79e11
Track Slab	Length/(m)	5
	Moment of Inertia /(N/m^2)	3.65e10
	Moment of Inertia /(m^4)	1.3718e-3
	Density /(kg/m^3)	2750
	Section area /(m^2)	0.456
Viaduct	Length/(m)	32
	Moment of Inertia /(N/m^2)	3.6e10
	Moment of Inertia /(m^4)	11.056
	Density /(kg/m^3)	2600
	Section area /(m^2)	2.205
Viaduct Bearing	Stiffness /(Pa)	6e9
	Distance between Bearings/(m)	32

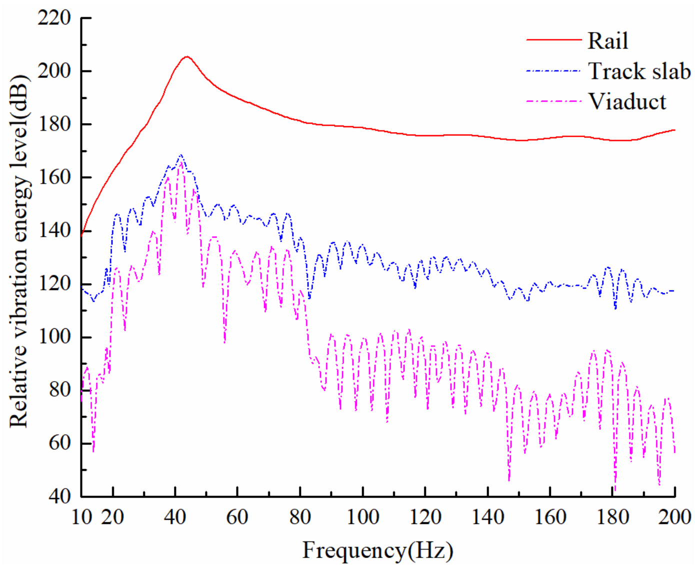

Fig. 5 Relative vibration energy level of normal conditions

for the vehicle-track-viaduct coupling model relies on the irregularity of the vertical rails of the track structure. According to the relevant settings of other scholarss (Xu *et al*. 2017) research on contact loss beneath the track slab, the distance of contact loss beneath track slab (the distance of the partial contact loss at one edge beneath track slab is from the left end to the middle of the track slab, and the distance of the partial contact loss at midpoint beneath track slab is from the middle to the ends of the track slab) are 0.31 m, 0.94 m, 1.56 m, 2.19 m, and 2.81 m. Figure 4 shows the calculation on conditions.

3.3 Analysis of track structure ınteraction system in partial contact loss at one edge beneath track slab

Applying the vehicle-track-viaduct coupling analysis and calculation model established above, the velocity for the carriage is taken as 300km/h (this speed is commonly used in high-speed trains in China). When the train is running at the mid-span position of the viaduct, the contact loss beneath the track slab end at different degrees and the vibration energy distribution and transmission of the track structure are calculated.

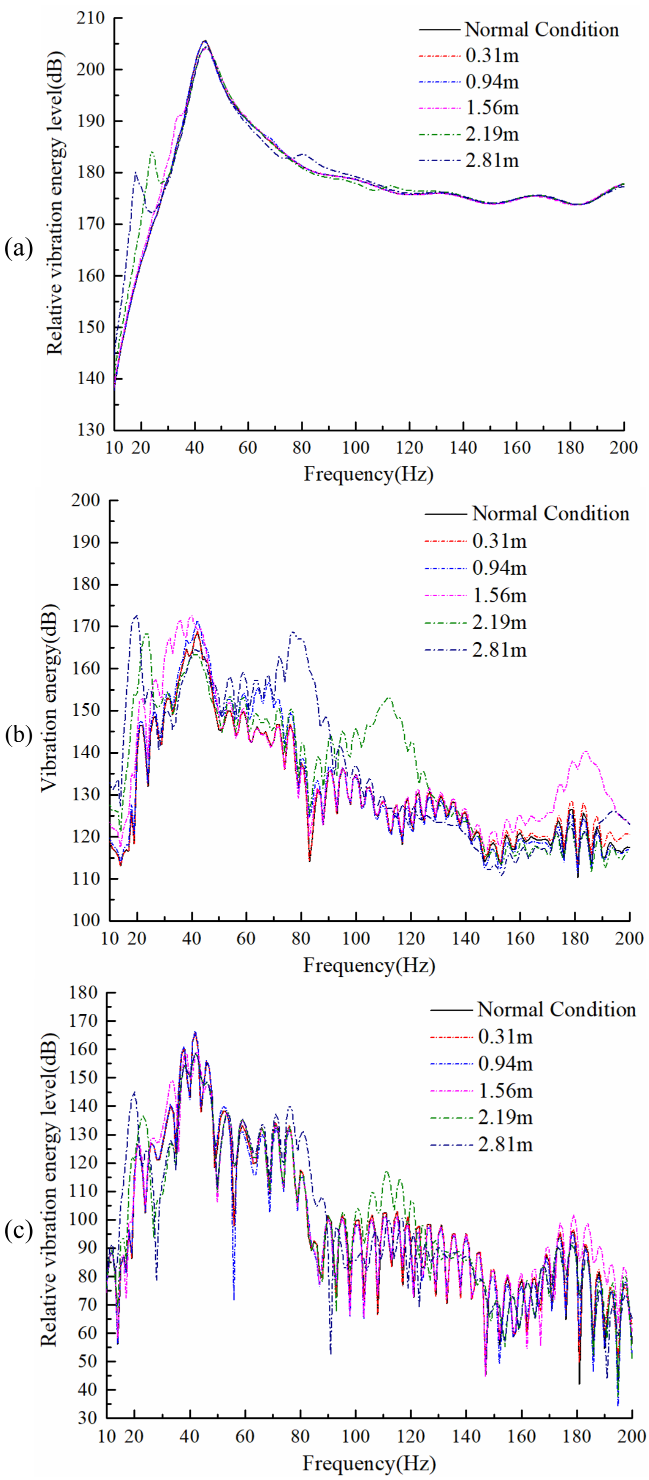

Fig. 6 Relative Vibration Energy Level of Partial Contact Loss at One Edge Beneath Track Slab (a) Rail; (b) Track slab; (c) Viaduct

3.3.1 Relative vibration energy level of partial contact loss at one edge beneath track slab

The study calculates the relative vibration energy level distribution of the track structure in [10, 200] Hz under normal conditions, shown in Figure 5.

From Figure 5, within this frequency range, the relative vibration energy levels of the various layers of the track structure (rail, track slab, viaduct) first increase and then decrease, and are at the maximum point at 45 Hz. The wheel-rail force is located at a similar frequency. This phenomenon occurs because the vibration energy generated after the wheel contacts the rail is continuously dissipated and gradually decreased during the vertical transmission from the rail to the track slab along the track structure.

Fig. 6(a-c) show that when the length is 1.56 m, the rails, track slab and viaduct all have sudden changes in vibration energy peaks and migration because, as the length of the partial contact loss at one edge beneath track slab increases, the overall stiffness of the track structure decreases. Specifically, as the length increases, the rail relative vibration energy level will have other peaks at lower frequencies when the dominant frequency peak is unchanged, and the peak will continue to move forward. At the track plate, the first main frequency of its relative vibration energy level is located at 42Hz, the peak value increases with the length of the contact loss beneath the track slab. The energy level increases significantly at a length of 0.94 m, reaching 117.48% of normal conditions at 2.81 m. The main frequency shifts forward and two obvious peaks appear. At a length of 2.81 m, the frequencies corresponding to the peaks are 21Hz, 42Hz, and 78Hz, respectively. At the viaduct, the change of the relative vibration energy level is like that of the track slab. Two obvious main peaks occur after 1.56 m, gradually moving forward with the change of the length of the contact loss beneath the track slab.

Similarly, the relative vibration energy levels of the track structures (rail, track plate, viaduct) at different lengths of contact loss beneath the track slab all appear as the frequency increases, first reaching a peak at 45 Hz, and then gradually decreasing. This phenomenon shows that the length does not have much influence on the dominant frequency of energy levels.

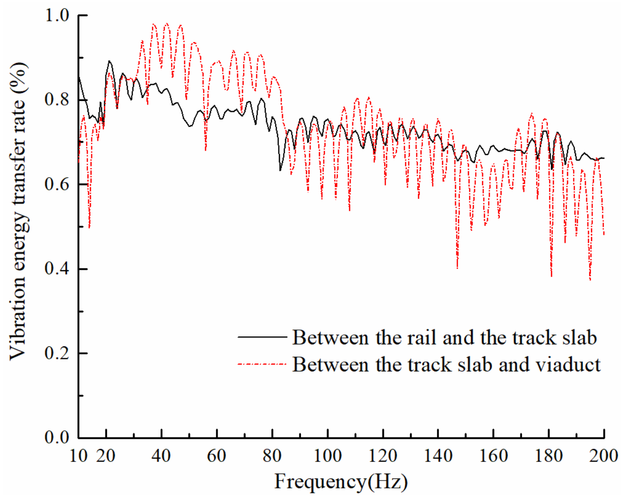

Fig.7 Vibration energy transfer rate of normal conditions

3.3.2 Vibration energy transfer rate of partial contact loss at one edge beneath track slab

By analyzing the vibration energy transfer rate situation of the track structure in normal conditions, the energy transfer from the rail to the track slab and the track slab to

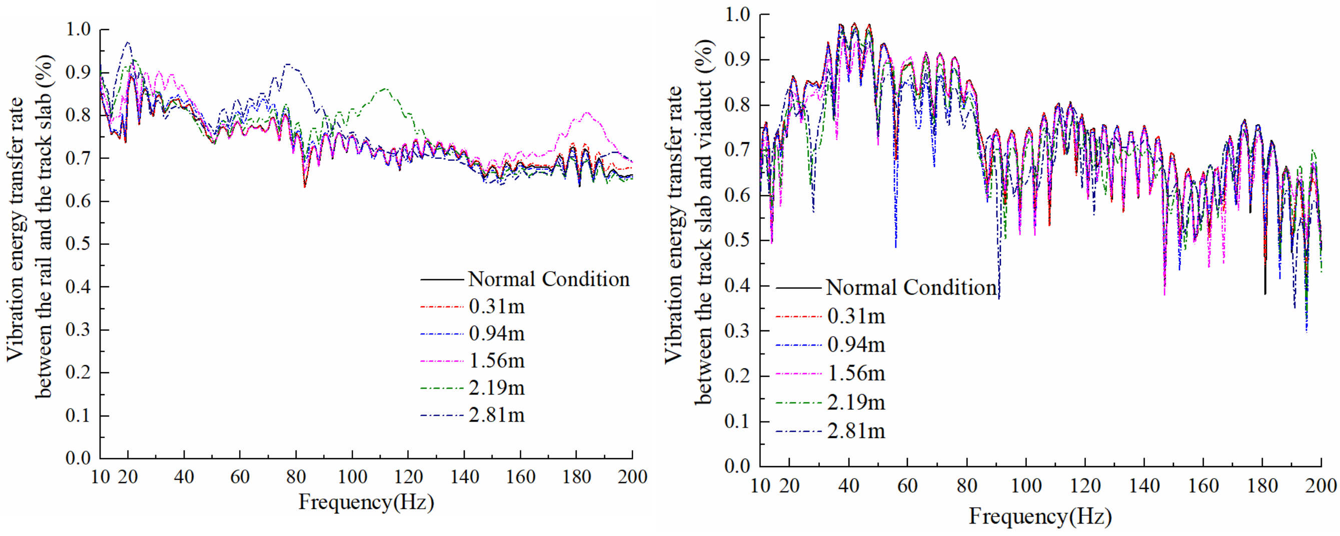

(a) (b)

Fig. 8 Vibration Energy Transfer Rate of Partial Contact Loss at One Edge Beneath Track Slab:(a) Vibration energy transfer rate between the rail and the track slab; (b) Vibration energy transfer rate between the track slab and viaduct

the viaduct can be intuitively recognized. It analyzes the changes in the energy transfer of the track structure and the corresponding hazards due to the contact loss beneath the track slab.

Fig. 7 shows that the vibration energy transfer rate from the rail to the track slab gradually decreases with increasing frequency under normal operating conditions, but it is concentrated around 0.76%. The vibration energy transfer rate from the track plate to the viaduct first increases and then decreases. The maximum value is 0.918%, which is 2.8% larger than the value between the rail and the track slab. After 84Hz, the rate shows repeated oscillations because of the combination of the elasticity and damping of the fastener, which causes the vibration energy between the rail and the track slab to gradually dissipate during the transfer.

Figure 8 shows that with the increase of the length of partial contact loss at one edge beneath track slab, the vibration energy transfer rate between the rail and the track slab increases significantly. After 1.56 m, the increase of the rate is significant, and a peak appears at 184Hz and continues to move forward as the length increases. This phenomenon occurs because, with the increase in the length of the contact loss beneath the track slab, the track structure is gradually weakened by the lateral support, which further causes the track plate to be in a cantilever position. This aggravates the track irregularity, and eventually, leads to the increase of the vibration energy transfer rate between the rail and the track slab. At 2.81 m, the rate from the rail to the track slab at 20Hz reaches 0.974%, which is an increase of 9.2% compared to normal conditions, reflecting that the contact loss beneath the track slab will intensify the energy distribution between the track and the track plate, affecting the service life of the track.

The vibration energy transfer rate from the track slab to the viaduct decreases with increasing length because of the contact loss beneath the track slab. The energy of the track slab at the vacancy, therefore, could not be transferred further downward but was diverted between the rail and the track slab. After 1.56 m, the rate was significantly reduced, and a multiple wave-trough appeared. At 2.81 m, the rate at 195Hz is 0.465%, which is far less than the normal condition.

3.4 Analysis of track structure ınteraction system in partial contact loss at midpoint beneath track slab

The analysis of the track structure interaction during partial contact loss at midpoint beneath track slab is the same as the analysis of the partial contact loss at one edge beneath track slab. The influence of partial contact loss at one edge beneath track slab on the track structure when the train is located at the mid-span position of the bridge is studied by using track irregular excitation.

3.4.1 Relative vibration energy level of partial contact loss at midpoint beneath track slab

When the running speed V is 300 km/h and the train is running at the mid-span position of the viaduct, the vibration energy distribution and transfer of the track structure under different degrees of disengaging in the track slab are analyzed.

Figure 9 shows that as the length of the partial contact loss at midpoint beneath track slab increases, the dominant frequency peak will migrate to a low frequency. When it reaches 1.56 m, the vibration energy of the rail layer at the dominant frequency peak at 167Hz significantly increases. When it reaches 2.81 m, the dominant frequency moves forward to 131Hz. Compared with the partial contact loss at one edge beneath track slab, the partial contact loss at midpoint beneath track slab has less effect on the vibration energy of the rail layer in the low frequency range, and the

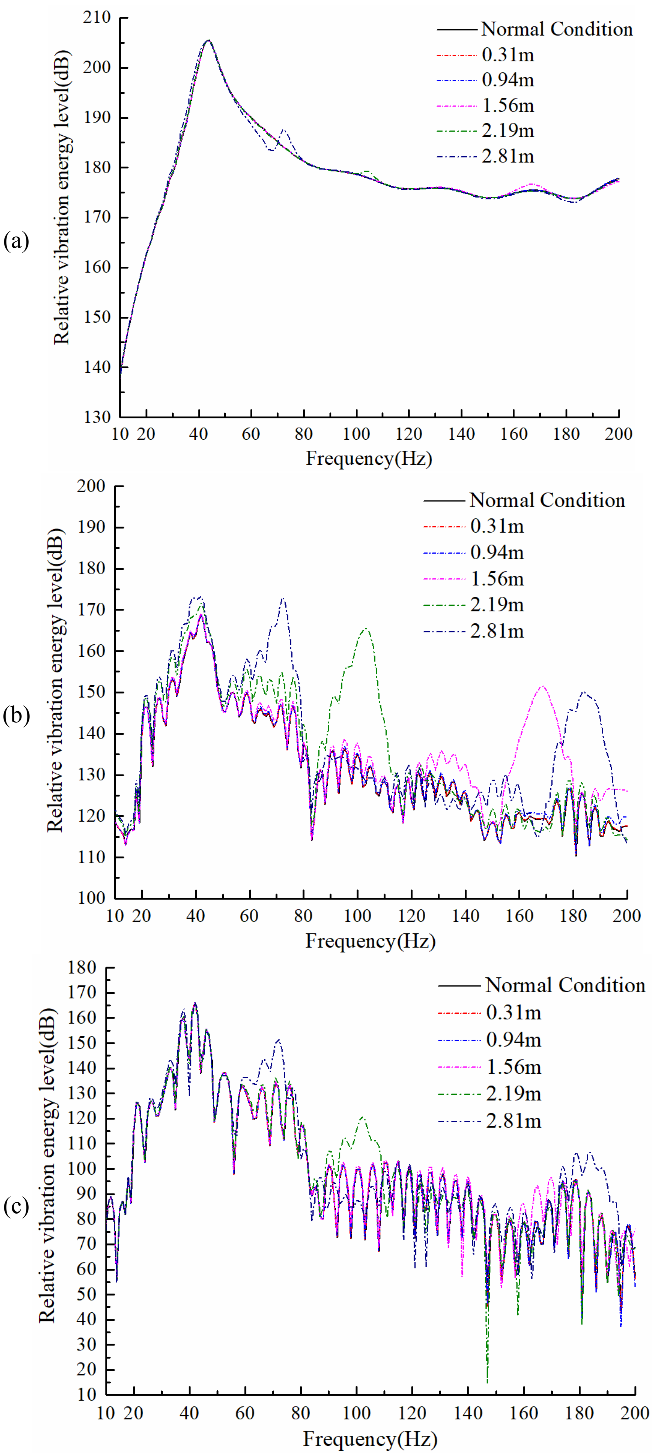

Fig. 9 Relative Vibration Energy Level of Partial Contact Loss at Midpoint Beneath Track Slab: (a) Rail; (b) Track slab; (c) Viaduct

peak value of the rail at the maximum dominant frequency does not change significantly with the increasing length. The relative vibration energy level at the track slab increased significantly after 1.56 m, and at 2.81 m, the maximum peak at 72Hz was 173dB, which was an increase of 17.9% compared to normal conditions. The change with the length of the viaduct is relatively small compared to the track slab, and the peak at the maximum dominant frequency does not change much. After the length reaches 2.19 m, a significant increase occurs in [55, 89] Hz. In [10, 60] Hz, the energy level of each layer of the track structure under the contact loss beneath the track slab middle is unaffected by the disengaging. In [60, 200] Hz, the vibration energy of various layers of the track structure fluctuates greatly. Specifically, the relative vibration energy level at the track slab is affected by the disengagement, causing energy aggregation.

3.4.2 Vibration energy transfer rate of partial contact loss at midpoint beneath track slab

In Figure 10, compared with the vibration energy transfer rate of the partial contact loss at one edge beneath track slab, the rate between the rail, and the track slab, the partial contact loss at midpoint beneath track slab does not change much at low frequencies, and jumps only in some frequency range. The rate between the track slab and the viaduct does not change much, reflecting that under the same length, the influence of the partial contact loss at midpoint beneath track slab on the overall structure of the track is smaller than the partial contact loss at one edge beneath track slab (Xu *et al*. 2017).

4. Conclusions

To evaluate the influence of contact loss beneath the track slab on the track structure as a whole, this paper adopts the power flow theory and analyzes the two main indexes of the power flow theory, namely the relative vibration energy level, and the vibration energy transfer rate. The comparative analysis of the vibration energy distribution and transmission characteristics of the rails, track slab, and viaduct layers in the track structure when the high-speed train runs to the mid-span position of the viaduct under normal conditions, contact loss appears beneath the track slab end and the track slab middle. The main conclusions are as follows:

1. When the partial contact loss is beneath the track slab, the relative vibration energy level between the rail and the track plate increases significantly in [10, 200] Hz. When the partial contact loss at one edge beneath track slab, the rail relative vibration energy level increases by 20dB, the track slab increases by 35dB, and little change exists in the level of the viaduct. This reflects that when the partial contact loss at one edge beneath track slab, vibration energy accumulates on the track slab of the adjacent to disengage, causing further damage to the track structure and seriously threatening safe driving.

2. When the partial contact loss at midpoint beneath track slab, it has little effect on the vibration energy of the rail and viaduct. As the length of the disengagement increases, the peak value of its maximum dominant frequency does not change much, but the vibration energy at the track slab changes significantly. After the length of disengaging is 1.56 m, the level increases significantly. When the length is 2.81 m, the maximum peak at 72Hz is 173dB, which is an increase of 17.9% compared to normal conditions.

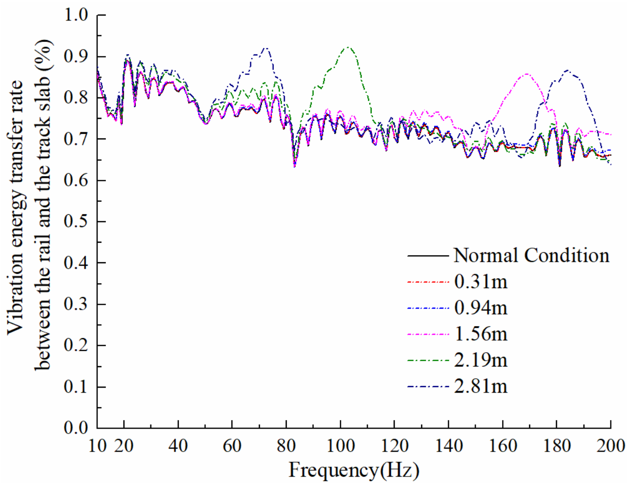

(a)

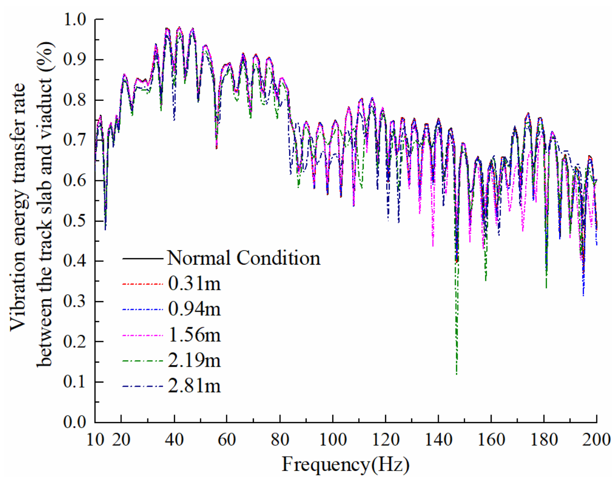

(b)

Fig. 10 Vibration Energy Transfer Rate of Partial Contact Loss at Midpoint Beneath Track Slab:(a) Vibration energy transfer rate between the rail and the track slab; (b) Vibration energy transfer rate between the track slab and viaduct

3. Comparing the two types of partial contact loss beneath the track slab at the same length, the relative vibration energy level and its vibration energy transfer rate between the rail and the rail plate at partial contact loss at one edge beneath track slab regarding partial contact loss at midpoint beneath track slab increase significantly. This is because, compared to the partial contact loss at midpoint beneath track slab, the track structure under the condition of partial contact loss at one edge beneath track slab loses the lateral support, which causes the track to be in a cantilever position, and the track irregularity intensifies, which seriously affects the service life of the rail.

Acknowledgement

This study is financially supported by National Natural Science Grant (No. 51578238, 51968025), Jiangxi Province Natural Science Grant for Key Projects (No. 20192ACBL20009), and Jiangxi Province Key Research and Development Fund (No. 20181BBE50013).

References

Carlone, L. and Thompson, D.J. (2001), "Vibration of a rail coupled to a foundation beam through a series of discrete elastic supports", SU ISVR TM-873; University of Southampton, United Kingdom.

Dai, G., Wang, M. and Liu, W. (2018), "Experimental study on deformation of CRTS II ballastless track-simply supported beam bridge under dynamic load", *J. Vib. Shock*, **37**(07), 102-108. https://doi.org/10.13465/j.cnki.jvs.2018.07.016.

Fu, N., Yu, L., Zhao, Z. and Li, C. (2018), "Study of vibration energy properties of double-block ballastless damping track", *J. China Railway Soc.,* **40**(10), 115-122. https://doi.org/ 10.3969/j.issn.1001-8360.2018.10.016.

Fenander, Å. (1997), "Frequency dependent stiffness and damping of railpads", *Proc. Institution of Mech. Eng., Part F J. Rail Rapid Transit*, **211**(1), 51-62. https://doi.org/10.1243/0954409971530897.

Hamet, J.F. (1999), "Railway noise: Use of the Timoshenko model in rail vibration studies", *Acta Acustica united with Acta Acustica united with Acustica, Acustica*, **85**(1), 54-62.

Kaewunruen, S. and Remennikov, A.M. (2007), "Investigation of free vibrations of voided concrete sleepers in railway track system", *Proc. Institution Mech. Eng.*, **221**(4), 495-507. https://doi.org/ 10.1243/09544097JRRT141.

Li, P., Liu, X. and Li, G. (2014), "Influence of CA mortar void on dynamic characteristics of unit slab track on bridge", *China Railway Sci.*, **35**(03), 20-27. https://doi.org/10.3969/j.issn.1001-4632.2014.0304.

Li, Z. and Wu, T. (2010), "Analysis of vibration power flow for a railway vehicle-track-viaduct coupled system", *J. Vib. Shock,* **29**(11), 78-82+93+254. https://doi.org/10.13465/j.cnki.jvs.2010.11.032.

Liu, H.P., Wu, T.X. and Li, Z.G. (2009), "Theoretical modeling and effectiveness study of rail vibration for noise control", *J. Sound Vib.,* **323**(3-5), 594-608. https://doi.org/10.1016/j.jsv.2009.01.036.

Liu, L., Qin, J., Zhou, Y., Xi, R. and Peng, S. (2019a), "Structural noise mitigation for viaduct box girder using acoustic modal contribution analysis", *Struct. Eng. Mech.,* **72**(04), 421-432. https://doi.org/10.12989/sem.2019.72.4.421.

Liu, L., Song, R., Zhou, Y. L. and Qin, J. (2019b), "Noise and vibration mitigation performance of damping pad under CRTS-III ballastless track in high speed rail viaduct", *KSCE J. Civil Eng.,* **23**(8), 3525-3534. https://doi.org/ 10.1007/s12205-019-1947-4.

Liu, L., Qin, J., Liu, Q., Yau, J.D. and Song, R. (2019c), "Spectral analysis of train-rail-bridge coupling system considering frequency-dependent stiffness of rail fastening systems", *J. Marine Sci. Technol.*, **27**(2), 114-122. https://doi.org/10.6119/JMST.201904_27(2),0004.

Liu, L., Lu, P. and Qin, J. (2019d), "Random vibration analysis of vehicle-track coupling system based on fastener FVMP model", *J. China Railway Soc.,* **41**(05), 93-100. https://doi.org/10.3969/j.issn.1001-8360.2019.05.011.

Ren, J., Li, X., Yang, R. Wang, P. and Xie, P. (2016), "Criteria for repairing damages of CA mortar for prefabricated framework-type slab track", *Construct. Building Mater.*, **110**, 300-311. https://doi.org/10.1016/j.conbuildmat.2016.02.036

Ren, J., Wang, J., Li, X., Wei, K., Li, H. and Deng, S. (2020), "Influence of cement asphalt mortar debonding on the damage distribution and mechanical responses of CRTS I prefabricated slab", *Construct. Build. Mater.*, **230**, 1-12. https://doi.org/10.1016/j.conbuildmat.2019.116995

Schulte-Werning, B., Beier, M. and Degen, K.G. (2006), "Research on noise and vibration reduction at DB to improve the environmental friendliness of rail- way traffic", *J. Sound Vib.,* **293**(3-5), 1058-1069. https://doi.org/10.1016/j.jsv.2005.08.065.

Shi, G., Yang J., Yang X., Zhang, X. (2017), "Vertical vehicle-track-bridge coupling vibration based on dynamic flexibility method", *J. Central South U.*, **48**(4), 1119-1126. https://doi.org/10.11817/j.issn.1672-7207.2017.04.036.

Song, R., Liu, L. Xu, B., Liu, Q., Qin, J. (2018), "Study on vibration reduction performance of rubber pads for track viaducts based on dynamic flexibility method", *Noise Vib. Control,* **38**(3), 141-145. https://doi.org/10.3969/j.issn.1006-1355.2018.03.027.

Song, X., Zhai, W. and Wang, S. (2012), "Vertical displacement distributions of ballastless track infrastructure of high-speed railways", *China Civil Eng. J.*, **45**(05), 162-168. https://doi.org/10.15951/j.tmgcxb.2012.05.007.

Sun, L., Duan, Y., Zhao, L. and Zhang, Y. (2014), "Dynamic characteristic analysis of CRTS II plate ballastless track structure of high speed railway", *J. Southeast University*, **44**(2), 406-412. https://doi.org/10.3969/j.issn.1001-0505.2014.02.032.

Thompson, D.J. and Verheij, J.W. (1997), "The dynamic behaviour of rail fasteners at high frequencies", *Appl. Acoustics*, **52**(1), 1-17. https://doi.org/ 10.1016/S0003-682X(97)00016-9.

Xu, H., Lin, K.Y. and Wang, P. (2017), "Effect analysis of CRTS Ⅰ type CA mortar degradation on its fatigue life", *J. Railway Eng. Soc.*, **34**(12), 31-34. https://doi.org/10.3969/j.issn.1006-2106.2017.12.007.

Zhu, Z., Gong, W., Zhang, L., Yu, Z. and Chengbiao, C. (2018), "An efficient hybrid algorithm for dynamic analysis of train-track-bridge coupled system based on separation iterative method and coupled time-varying method", *China Railway Sci.*, **39**(01), 66-74. https://doi.org/10.3969/j.issn.1001-4632.2018.01.09.

CC